

NUMERICAL SIMULATION OF COMBUSTION PROCESS OF LEATHER RESIDUALS GASIFICATION GAS

Cristiano Vitorino da Silva, cristiano@uricer.edu.br

Arthur Bortolin Beskow, arthur@uricer.edu.br

Department of Engineering and Computational Science, Universidade Regional Integrada do Alto Uruguai e das Missões - URI.
GEAPI – Group of Applied Engineering to Industrial Processes.
LABSIM – Numerical Simulation Laboratory.

Maria Luiza Sperb Indrusiak, mlsperb@unisinis.br

Mechanical Engineering Department, Universidade do Vale do Rio dos Sinos – UNISINOS.

Nilson Romeu Marcilio, nilson@enq.ufrgs.br

Chemical Engineering Department, Universidade Federal do Rio Grande do Sul - UFRGS.

Marcelo Godinho, godinho@enq.ufrgs.br

Chemical Engineering Department, Universidade Federal do Rio Grande do Sul – UFRGS.

Abstract. *This work presents a numerical study of combustion process of leather residual gasification gas, aiming the improvement of the efficiency of the gas burning process. The thermal energy produced can be used to generation of energy, thermal and/or electric, for use at the leather industrial plant. However, the direct burning of this leather-residual-gas into the chambers is not a simple process. An alternative to be developed consist in to process this leather residuals by gasification or pyrolysis, separate the volatiles and incomplete products of combustion, for after use as fuel in a boiler. Yet another problem related to the burning of gas-product of leather-gasification is the presence of environment-harmful-gases, remainings of the chemical treatment employed at leather manufacture, as cyanide, hydrocarbons as the toluene, the chrome and other toxic gases, as the carbon monoxide and NO_x , that must be either fully consumed in combustion process, or have their production minimized, with the purpose of reduce the emission of pollutants into the atmosphere. At this way, aiming a better understanding of the combustion process and in order to obtain improved design of this kind of furnace, it was made a numerical simulation study of reactive flow in the chamber, for evaluate the thermal changes, the chemical reactions rates at the process and the flow field as well. The commercial CFD software CFX © Ansys Inc. was used. This kind of computational tool achieve good results at low costs and time. Beyond that, with the improvement of computational technology, is possible to predict large quantities of details, obtaining solutions closer to the actual operation conditions, helping significantly the analysis of new designs of devices and equipments.*

Keywords: *Leather, CFD, Combustion, Finite Volumes, Waste to Energy.*

1. INTRODUCTION

The development of feasible technologies in order to make profitable the use of nonconventional energy sources in replacement of fossil fuels is one of the biggest technological challenges of the present times. The main reasons for that are the global warming associated with fossil fuels combustion emissions and the finite reserves of those fuels.

There are many industries dedicated to the production of leather clothes, handbags and shoes at Brazilian southeast region. Due to its origin, availability and thermal value, the leather waste is considered a biomass fuel. Other favorable result of the combustion of leather is the ash by-product. They are rich in chromium and can be used as raw material in the steel industry for the production of Fe-Cr alloys. They can be also recycled into chromium sulphate which is used in the tanning process. The chromium acid, used in electroplating, is another possible application (Godinho, 2006). Beyond that, another big problem that mankind must learn how to cope with is the final destination of waste. The usual disposal in landfills is no more acceptable due to harmful consequences as underground water contamination and methane emissions due to the decomposition process of the organic raw material. The allocation of large ground areas for waste disposal is also an emerging problem. Albeit, direct burning of biomass is not straightforward due to many technical and environmental requirements. As a consequence, several techniques are being studied, e.g. the collection and use of methane in energy production plants, composting, anaerobic digestion, and combustion or gasification of the waste. They are called waste to energy (WtE) technologies and present large possibilities for improvements. The knowledge of the technologies of gasification and combustion of biomass is not completely developed and many research studies were done in the last years mainly related to coal, waste and biomass. Nevertheless, studies related to leather residues are very rare.

The efficient operation of combustion chambers of gasifiers and boilers is strongly dependent upon the oxidation reactions and heat, mass and momentum transfers occurring inside the devices. Therefore, improvements to the project

of those devices are welcome. A substantial quantity of works about biomass combustion can be found in the literature, albeit few of them are related to leather combustion or gasification.

Bahillo *et al.* (2004) performed experimental studies on fluidized bed combustion of leather scraps. The HCN and NH₃ concentrations were measured in the reactor core and at the flue gas. According to the results, the concentrations are very low at flue gases; nevertheless they are high at the reactor core. The HCN concentration is considerably higher than that of NH₃.

Godinho *et al.* (2006) presented an experimental analysis of a semi-pilot plant for the processing of footwear leather wastes. The objective of the work was to evaluate the performance of the plant. The unit comprises a stratified downdraft gasifier, an oxidation reactor and an air pollution control system (APC). The results obtained in this work led to conclude that the operational conditions applied in the process provided a low degree of oxidation of the chromium content in the waste. There is also a significant participation of water-soluble compounds in the particulate matter. The low concentration of CO in the flue gas indicates high combustion efficiency for the process. A significant reduction of the NO emissions was obtained, compared to the results of the combustion of footwear leather waste in fluidized bed. The main conclusion is that the footwear leather waste (biomass) represents an alternate source for the generation of electric energy. In another work, Shin *et al.* (2008) presents an investigation about the combustion characteristics of gas fuel in a pyrolysis-melting incinerator. The study aims to develop a novel incineration process considering the intrinsic characteristics of waste generated in Korea. The effects of secondary and tertiary air on flow pattern, mixing, and NO_x emissions of the combustion chamber were investigated. The pyrolyzed gas was simulated by propane, a mid-sized molecule among all the components. The propane was injected in the combustion chamber, and burnt through multi-step combustion by distributing the combustion air to primary, secondary, and tertiary air nozzles. Temperature and gas components in the combustion performances were determined by temperature distribution and O₂, CO and NO_x chemical species concentration. These results conclude that using the secondary and/or tertiary air, the combustion performance was improved, and, in particular, NO_x concentration decreased significantly following the tertiary air injection.

Salvador *et al.* (2006) presented a numerical 2D model to simulate the coupled equations for flow, heat transfer, mass transfer and progress of chemical reactions of a thermal recuperative incinerator (TRI) used to oxidize volatile organic compounds (VOCs) diluted in an air flow. The commercial software Fluent (Fluent Inc., 1998) was used. This model was confronted with experimental values obtained on a highly instrumented semi-industrial-scale pilot unit running under the same conditions. The results show that the model developed is a good tool for the analysis of combustion processes and it can predict important information about the flow, heat transfer and pollutant formation.

The work of Choi and Yi (2000) presented a numerical study of a combustion process of VOCs in a regenerative thermal oxidizer (RTO). Steady and unsteady flow field, distributions of temperature, pressure and compositions of the flue gas in the RTO were simulated by computational fluid dynamics (CFD) using the commercial software Fluent (Fluent Inc., 1998). The model system was the oxidation of benzene, toluene and xylene by the RTO, which was constituted by three beds packed with ceramic beads to exchange heat. The results show that a level of 1.0% of VOCs is sufficient to provide energy for the oxidation when heat is exchanged through the ceramic bed. A ceramic bed of 0.2 m in height is sufficient to operate properly at these conditions and 5 s is recommended as the stream switching time. In addition, the results can provide insight and practical responses involved in the design of an industrial RTO unit.

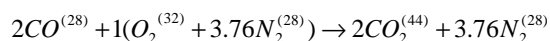
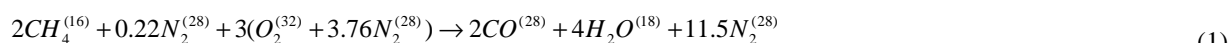
The present research work presents a numerical simulation study, using a commercial CFD code, applied to the development of an optimized design of furnace used to burn the resulting gas of the leather gasification process. The subject of the study is the analysis of combustion processes of the gas, the verification of the effect of the gas flow along the combustion chamber of a furnace of an industrial unit pilot. The main objectives are to verify the global efficiency of the burning process and to provide insight related to mechanical of the flow inside the chamber.

2. MATHEMATICAL FORMULATION

The proposed task can be stated as follows: design a combustion chamber to burn leather residual gasification gas in air, compute the temperature, chemical species concentrations and the velocity fields for gas mixture, and verify geometry features on the combustion process and pollutant formation.

The chemical reaction of the leather residual gasification gas used at this work, that here is considered composed to HCN, methane, hydrogen and carbon monoxide, is modeled according to global equations presented on Westbrook and Dryer (1981), which follow:

The methane oxidation is modeled by two global steps, given by:



The carbon monoxide oxidation is modeled by:



The hydrogen oxidation is modeled by:



The formation of NO_x is modeled by Zeldovich mechanisms using two different paths, the thermal-NO and the prompt-NO, where the first, that is predominant at temperatures above 1800 K, is given by tree-step chemical reaction mechanisms:



In sub or near stoichiometric conditions, a third reaction is also used



where the chemical reaction rates are predicted by Arrhenius equation.

The prompt-NO is formed at temperatures lower than 1800 K, where radicals can react rapidly with molecular nitrogen to form HCN, which may be oxidized to NO under flame conditions. The complete mechanism is not straightforward. However, De Soete proposed a single reaction rate to describe the NO source by Fennimore mechanism, which is used at this work, and the Arrhenius equations are used for predict this chemical reaction rate. At this way, the HCN oxidation to form NO is modeled by:



The HCN oxidation to consume the NO is



The HCO oxidation is modeled by



And, to the reburn of NO by the CH_4 fuel gas:



Scalar transport equations are solved for velocity, pressure, temperature and chemical species. The bulk motion of the fluid is modeled using single velocity, pressure, temperature, chemical species and turbulence fields.

2.1. Mass and species mass fraction transport equations

Each component has its own Reynolds-averaged equation for mass conservation, which, considering incompressible and stationary flow can be written in tensor notation as a mixture fraction of all components. So, the standard continuity equation can be written as

$$\frac{\partial \left(\tilde{\rho}_i \tilde{U}_j \right)}{\partial x_j} = 0 \quad (8)$$

where $\tilde{U}_j = \sum \left(\tilde{\rho}_i \tilde{U}_{ij} \right) / \bar{\rho}$, $\tilde{\rho}_i$ and $\bar{\rho}$ are respectively the mass-average density of fluid component i in the mixture

and the average density, x is the spatial coordinate, and \tilde{U}_{ij} is the mass-averaged velocity of fluid component i .

The mass fraction of component i is defined as $\tilde{Y}_i = \tilde{\rho}_i / \bar{\rho}$. Substituting this expressions into Eq. (8) and modeling the turbulent scalar flows using the eddy dissipation assumption it follows that

$$\frac{\partial}{\partial x_j} \left(\bar{\rho} \tilde{U}_j \tilde{Y}_i \right) = \frac{\partial}{\partial x_j} \left(\left(\rho D_i + \frac{\mu_t}{Sc_i} \right) \frac{\partial \tilde{Y}_i}{\partial x_j} \right) + S_i \quad (9)$$

where D_i is the kinematic diffusivity, μ_t is the turbulent viscosity and Sc_i is the turbulent Schmidt number. Note that the sum of component mass fractions over all components is equal to one.

2.2. Momentum transport equations

For the fluid flow the momentum conservation equations are given by:

$$\frac{\partial}{\partial x_j} \left(\bar{\rho} \tilde{U}_i \tilde{U}_j \right) = -\frac{\partial p^*}{\partial x_j} \delta + \frac{\partial}{\partial x_j} \left(\mu_{eff} \frac{\partial \tilde{U}_i}{\partial x_j} \right) + \frac{\partial \tilde{U}}{\partial x_j \partial x_i} + S_U \quad (10)$$

where $\mu_{eff} = \mu + \mu_t$, and μ is the mixture dynamic viscosity and μ_t is the turbulent viscosity, defined as $\mu_t = C_\mu \bar{\rho} k^2 / \varepsilon$. The term $p^* = \bar{p} - (2/3)k$ is the modified pressure, C_μ is an empirical constant of the turbulence model, \bar{p} is the time-averaged pressure of the gaseous mixture, and δ is the Krönecker delta function. S_U is the source term, introduced to model the buoyancy and drag force due to the transportation particles, and other mathematical terms due to turbulence models. The Boussinesq model is used to represent the buoyancy force due to density variations.

2.3. The $k - \omega$ turbulence model

The equations for turbulent kinetic energy, k , and its turbulent frequency, ω , are:

$$\frac{\partial}{\partial x_j} \left(\tilde{\rho} \tilde{U}_j k \right) = \left(\frac{\partial}{\partial x_j} \left(\mu + \frac{\mu_t}{\sigma_k} \right) \frac{\partial k}{\partial x_j} \right) + P_k - \beta' \rho k \omega \quad (11)$$

$$\frac{\partial}{\partial x_j} \left(\tilde{\rho} \tilde{U}_j \omega \right) = \left(\frac{\partial}{\partial x_j} \left(\mu + \frac{\mu_t}{\sigma_\omega} \right) \frac{\partial \omega}{\partial x_j} \right) + \alpha \frac{\omega}{k} P_k - \beta \rho \omega^2 \quad (12)$$

where β' , β and α are empirical constants of the turbulence model, σ_k and σ_ω are the Prandtl numbers of the kinetic energy and frequency, respectively, and P_k is the term who accounts for the production or destruction of the turbulent kinetic energy.

$$P_k = \mu_t \left(\frac{\partial U_i}{\partial x_j} + \frac{\partial U_j}{\partial x_i} \right) \quad (13)$$

2.4. Energy transport equations

Considering the transport of energy due to the diffusion of each chemical species, the energy equation can be written as

$$\frac{\partial}{\partial x_j} \left(\tilde{\rho} \tilde{U}_j \tilde{h} \right) = \frac{\partial}{\partial x_j} \left(\left(\mu + \frac{\mu_t}{Pr_t} \right) \frac{\partial \tilde{h}}{\partial x_j} + \sum_i^{Nc} \tilde{\rho} D_i \tilde{h}_i \frac{\partial \tilde{Y}_i}{\partial x_j} + \frac{\mu_t}{Pr_t} \frac{\partial \tilde{h}}{\partial x_j} \right) + S_{rad} + S_{rea} \quad (14)$$

where \tilde{h} and c_p are the average enthalpy and specific heat of the mixture. The latter is given by $c_p = \sum_\alpha \tilde{Y}_\alpha c_{p,\alpha}$, where $c_{p,\alpha}$ and \tilde{Y} are the specific heat and the average mass fraction of the α -th chemical species, κ is the thermal conductivity of the mixture, Pr_t is the turbulent Prandtl number, and S_{rad} and S_{rea} represent the sources of thermal energy due to the radiative transfer and to the chemical reactions. The term S_{rea} can be written as:

$$S_{rea} = \sum_\alpha \left[\frac{h_\alpha^0}{MM_\alpha} + \int_{\tilde{T}_{ref,\alpha}}^{\tilde{T}} c_{p,\alpha} d\tilde{T} \right] \bar{R}_\alpha \quad (15)$$

where \tilde{T} is the average temperature of the mixture, h_α^0 and $\tilde{T}_{ref,\alpha}$ are the formation enthalpy and the reference temperature of the α -th chemical species. To complete the model, the density of mixture can be obtained from the ideal gas equation of state (Kuo, 1996; CFX Inc., 2004; Turns, 2000), $\bar{\rho} = p \overline{MM} \left(\bar{RT} \right)^{-1}$, where p is the combustion chamber operational pressure, which is here set equal to 1 atm (Spalding, 1979), and \overline{MM} is the mixture molecular mass. The aforementioned equations are valid only in the turbulent core, where $\mu_t \gg \mu$. Close to the wall, the logarithmic law of the wall is used (Launder and Sharma, 1974).

To consider thermal radiation exchanges inside the combustion chamber, the Discrete Transfer Radiation Model - DTRM is employed (Carvalho *et al.*, 1991), considering that the scattering is isotropic. The effect of the wavelength dependence is not considered, and the gas absorption coefficient is considered uniform inside the combustion chamber

and its value is 0.5 m^{-1} . Then, the Radiative Transfer Equation – RTE is integrated within its spectral band and a modified RTE can be written as

$$\frac{dI(r, s)}{dS} = \frac{K_a \sigma \tilde{T}^4}{\pi} - K_a I(r, s) + S'' \quad (16)$$

At the equations above, σ is the Stefan-Boltzmann constant ($5.672 \times 10^{-8} \text{ W/m}^2\text{K}^4$), r is the vector position, s is the vector direction, S is the path length, K_a is the absorption coefficient, I is the total radiation intensity which depends on position and direction, and S'' is the radiation source term, which can incorporate the radiation emission of the particles, for example.

2.5. The E-A (Eddy Breakup – Arrhenius) chemical reactions model

The reduced chemical reactions model that is employed here assumes finite rate reactions and a steady state turbulent process to volatiles combustion. In addition, it is considered that the combined pre-mixed and non-premixed oxidation occurs in two global chemical reaction steps, and involves the follow species: oxygen, methane, hydrogen, nitrogen, water vapor, carbon dioxide and carbon monoxide. A conservation equation is required for each species, with the exception of nitrogen. Thus, one has the conservation equation for the α -th chemical species, given by Eq. (9), where the source term, S_i , considers the average volumetric rate of formation or destruction of the α -th chemical species at all chemical reactions. This term is computed from the summation of the volumetric rates of formation or destruction in all the k -th equations where the α -th species is present, $\overline{R_{\alpha,k}}$. Thus, $\overline{R_{\alpha}} = \sum_k \overline{R_{\alpha,k}}$.

The rate of formation or destruction, $\overline{R_{\alpha,k}}$, can be obtained from an Arrhenius kinetic rate relation, which takes into account the turbulence effect, such as Magnussen equations (Eddy Breakup) (Magnussen and Hjertager, 1976), or a combination of the two formulations, the so called Arrhenius-Magnussen model (Eaton *et al.*, 1999; CFX Inc., 2004). Such relations are appropriate for a wide range of applications, for instance, laminar or turbulent chemical reactions with or without pre-mixing. The Arrhenius equation can be written as follows:

$$\overline{R_{\alpha,k,Chemical}} = -\eta_{\alpha,k} \overline{MM_{\alpha}} T^{-\beta_k} A_k \Pi_{\alpha} \overline{C_{\alpha}}^{\gamma_{\alpha,k}} \exp\left(\frac{-E_k}{RT}\right) \quad (17)$$

where β_k is the temperature exponent in each chemical reaction k , which is obtained empirically together with the energy activation E_k and the coefficient A_k . Π_{α} is the product symbol, $\overline{C_{\alpha}}$ is the molar concentration of the α -th chemical species, $\gamma_{\alpha,k}$ is the concentration exponent in each reaction k , \overline{R} is the gas constant, $\overline{MM_{\alpha}}$ and $\eta_{\alpha,k}$ are the molecular mass and the stoichiometric coefficient of α in the k -th chemical reaction.

In the Eddy-Breakup or Magnussen model, the chemical reaction rates are based on the theories of vortex dissipation in the presence of turbulence. Thus, for diffusive flames:

$$\overline{R_{\alpha,k,EBU}} = -\eta_{\alpha,k} \overline{MM_{\alpha}} A \rho \frac{\overline{\varepsilon}}{k} \frac{\overline{Y_{\alpha'}}}{\eta_{\alpha',k} \overline{MM_{\alpha'}}} \quad (18)$$

where the index α' represents the reactant α that has the least value of $\overline{R_{\alpha,k,EBU}}$.

In the presence of premixing, a third relation for the Eddy Breakup model is necessary, so that

$$\overline{R_{\alpha,k,Premixing}} = \eta_{\alpha,k} \overline{MM_{\alpha}} A B \rho \frac{\overline{\varepsilon}}{k} \frac{\sum_p \overline{Y_p}}{\sum_p \eta_{p,k} \overline{MM_p}} \quad (19)$$

where the index p represents the gaseous products of the combustion. A and B are empirical constants that are set as 4 and 0.5 (Magnussen and Hjertager, 1976). Magnussen model, Eqs. (18) and (19), can be applied to both diffusive and pre-mixed flames, or for the situation where both flames coexist, taking the smallest rate of chemical reaction.

Finally, for the Arrhenius-Magnussen model, given by Eqs. (17), (18) and (19), the rate of formation or destruction of the chemical species is taken as the least one between the values obtained from each model. It follows that

$$\overline{R_{\alpha,k}} = \min\left(\overline{R_{\alpha,k,Chemical}}, \overline{R_{\alpha,k,EBU}}, \overline{R_{\alpha,k,Premixed}}\right) \quad (20)$$

3. FURNACE DESCRIPTION

The furnace is a model already used for experimental studies and comprises four tubular segments. The segments are made of refractory concrete. The first two and the fourth segments have a coaxial external tube (jacket) that creates an annular region where air is preheated. The combustion chamber comprises the first segment of the furnace, where a mixture of primary air and fuel is injected. The secondary air is forced by a blower from the inlet at the upper region of the second segment through the annular tube and is injected into the combustion chamber by means of several small holes evenly distributed along the first segment. The auxiliary air that enters at the lower part of the fourth segment is preheated at the annular region, then premixed with fuel oil and injected through the two auxiliary burners (Fig. 1) during the startup of the plant. After the startup period, the auxiliary burners act as tertiary air feeders.

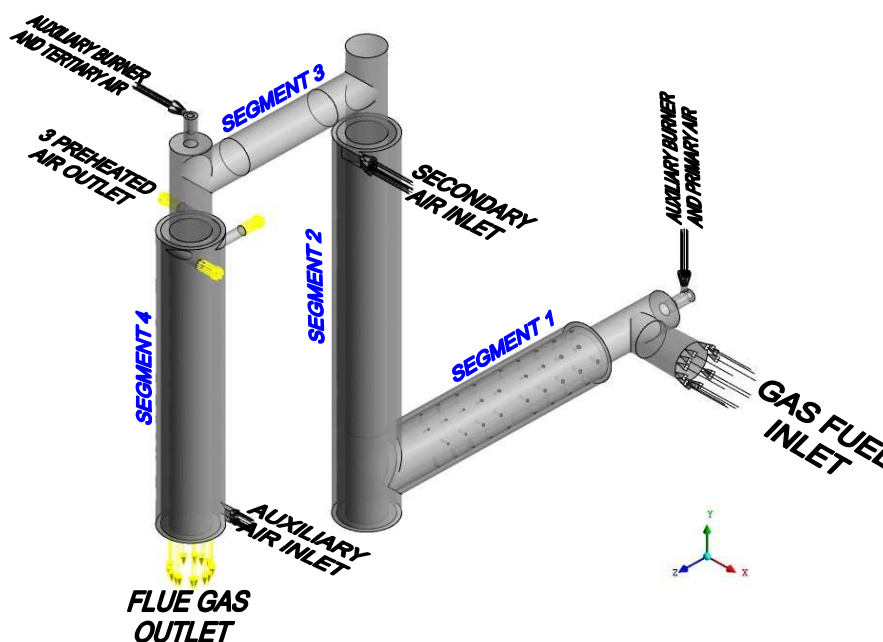


Figure 1 - General disposition of the furnace.

4. MESH SETTINGS AND CONVERGENCE CRITERIA

The domain under consideration comprises the furnace of a gasification/combustion plant to convert biomass in energy: the furnace comprises a tubular riser where occurs the combustion process of residual gasification gas as showed at Fig. 1. The entrance to furnace was considered the outlet of the domain. The discretization was done using tetrahedral volumes. Prismatic volumes were used at the walls in order to capture the boundary layer behavior and mesh refinements in the entrance region, corresponding to the first part of furnace. Due to computational limitations, the mesh size used has approximately 2.8×10^6 elements. The convergence criterion adopted was the RMS – Root Mean Square of the residual values, and the value adopted was 1×10^{-6} for all equations.

5. BOUNDARY CONDITIONS

In order to simulate the leather waste gasification gas, a fuel compounded of H_2O , N_2 , CO , HCN , CO_2 , H_2 and CH_4 was used. The species concentrations attributed to the fuel are shown in Tab. 1. It was considered that the mass flow rate of this gas is 740 kg/h at uniform inlet temperature of 800 °C. This temperature value was set considering the heating on gasification process.

The composition of the air for the combustion process was the usual one (23% of O_2 and 77% of N_2). The temperature of inlet secondary air is 25 °C, the same temperature of ambient air around the plant, and its mass flow rate is 720 kg/h. The inlet air in the auxiliary burners (primary and tertiary air) is heated in the pre-heater at segment 4, and its mass flow rate is 90 kg/h for each burner. Also, it was considered that the insulation used at the furnace wall has a thermal conductivity of approximately 1.4 W/mK and its density is 2300 kg/m^3 . It was not considered at this simulation the thermal resistance of the metallic walls.

Table 1 – Chemical composition of inlet fuel gas.

	Mass fraction	Mass flow [kg/h]		Mass fraction	Mass flow [kg/h]
H_2O	0.076	56.24	CO_2	0.230	170.20
O_2	-	-	H_2	0.007	5.18
N_2	0.642	475.08	CH_4	0.012	8.88
CO	0.032	23.68	HCN	0.001	0.74

6. RESULTS

The simulation showed that the design proposed for the furnace presented good combustion efficiency. Table 2 presents the bulk chemical composition of the flue gas at the furnace outlet, obtained with simulation process.

Table 2 – Bulk chemical composition of outlet flue gas.

	Mass Flow (kg/h)	Mass fraction		Mass Flow (kg/h)	Mass fraction
CH ₄	0.000009	0.0055 (ppm)	O ₂	117.330000	6.87 (%)
CO	0.000019	0.0110 (ppm)	NO	0.426300	249.60 (ppm)
CO ₂	245.300000	14.3600 (%)	N ₂	1215.300000	71.16 (%)
H ₂	0.000006	0.0030 (ppm)	HCO	0.000451	0.26 (ppm)
H ₂ O	129.280000	7.5700 (%)	HCN	0.158000	92.40 (ppm)

Figure 2-a shows the temperature field at a longitudinal plane. The flame core temperatures are of the order of 1700 °C, resulting in a more efficient combustion and less pollutants in flue gases. Figure 2-b shows the hydrogen concentration at the same longitudinal plane. Hydrogen is fully oxidized at the first half part of the furnace first segment. This led to the conclusion that the combustion chamber size is appropriate to the applied operational parameters.

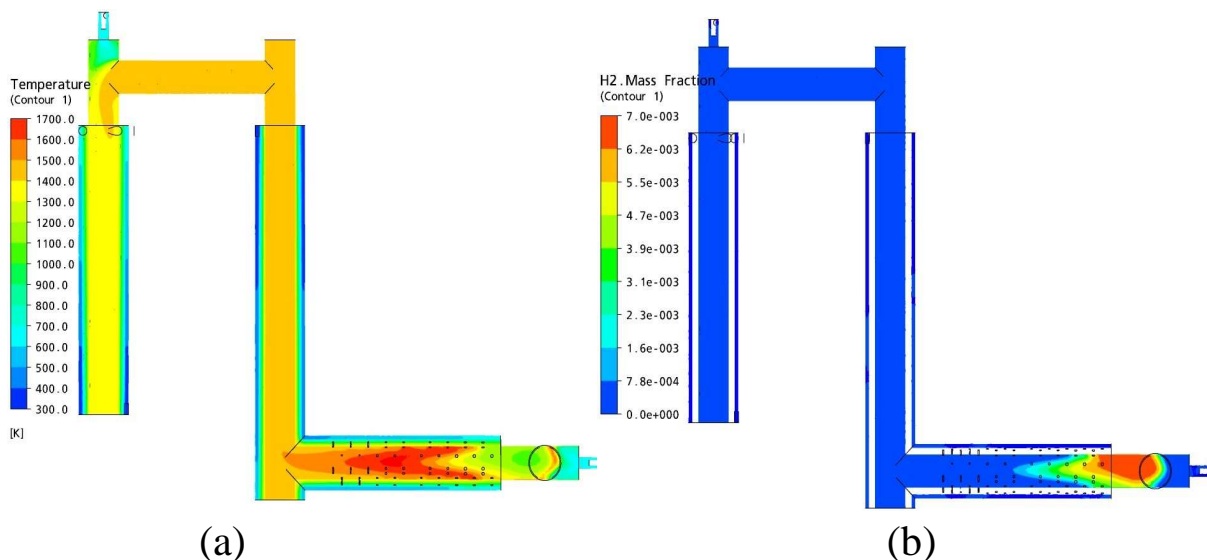


Figure 2 – (a) Temperature field; (b) Hydrogen concentration.

Figure 3 presents the temperature profiles at the combustion chamber (first segment) along with the temperature, velocity and mass flow rate values at the air feeders along the chamber. The main purpose of that air flow is to provide the excess air to ensure the complete gas combustion. One can observe that the air entering through the feeders penetrates the flame region and disturbs the temperature field but do not destabilize the flame.

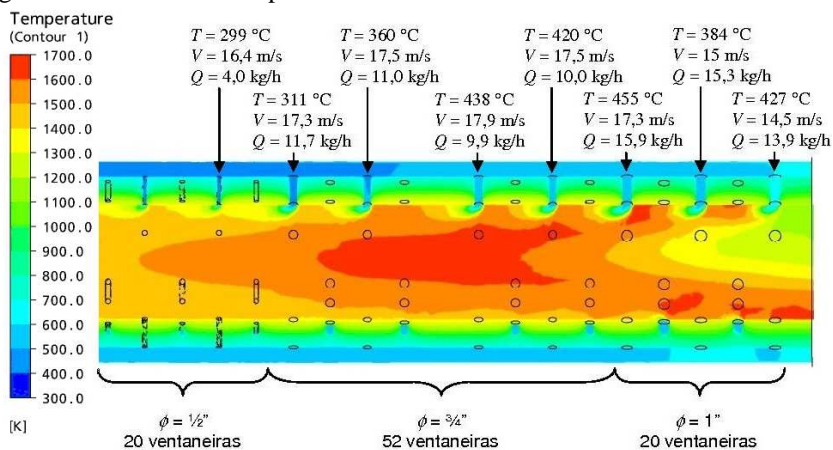


Figure 3 – Temperature profile at the combustion chamber and air feeders.

As observed in Fig. 3, the flame profile is not homogeneous along the chamber, instead concentrates along the core. This is due to the distorted mixture (air plus gas) flow at the combustion chamber up-flow region, determined by the furnace inlet design (Fig. 1). There is also a substantial increase of the secondary air temperatures along the jacket, thus the higher temperature air is fed at the beginning of the combustion process. This maintains high flame temperatures and enhances the burning process efficiency due to mixing promotion (tangential inlet) and oxygen supply. Figure 3 also shows that, as designed by assigning diverse values for the inlet diameters, the air velocities and mass flows at the feeders is not uniform.

Figure 4 presents the air flow characteristic streamlines at the combustion chamber jacket, showing again that the air distribution would not be homogeneous due to the spiral path of the flow. As a consequence, the mixing and the heat transfer are enhanced.

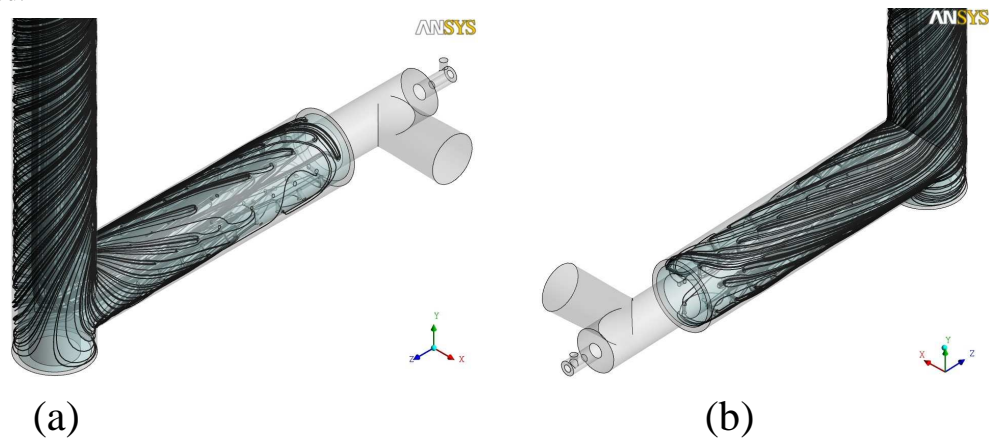


Figure 4 – Streamlines of the air flow in the pre-heating jacket: (a) front view; (b) rear view.

Figures 5-a and 5-b show the resulting concentration fields for CO and CH₄. The results of Fig. 2-b, 5-a and 5-b allow the conclusion that all the combustible is oxidized in the first half part of the combustion chamber (segment 1) and the resulting flame occupies all the combustion chamber segment.

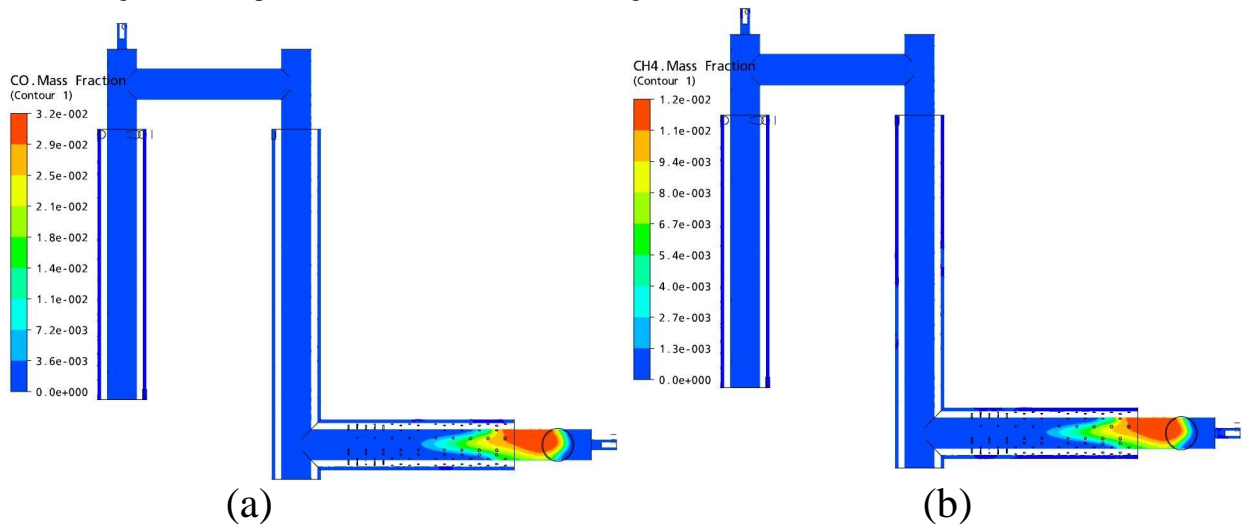


Figure 5 – (a) Carbon monoxide concentration; (b) Methane concentration.

Figures 6-a and 6-b show the resulting concentration field for oxygen and water vapor. Figure 6-a shows also that the higher oxygen concentrations are at the primary air inlet and progressively vanishes along the chamber, consumed by the combustion processes.

Figures 7-a and 7-b show respectively the concentration profiles of HCO and nitrogen along the furnace. The simultaneous observation of Fig. 2-a (temperature field) and 7-a (HCO field) enables the verification that the HCO production occurs at the higher temperatures region at the combustion chamber that comprises the flame tail. It is also observed that the HCO is completely oxidized along the combustion chamber.

The concentration field of HCN and NO_x (thermal + prompt + fuel) were presented at Fig. 8-a and 8-b. The higher HCN concentrations are also at segment 1, as expected – region of high hydrogen concentration (see Fig. 2-b). In the next segments the combustion products are diluted with the secondary and tertiary air.

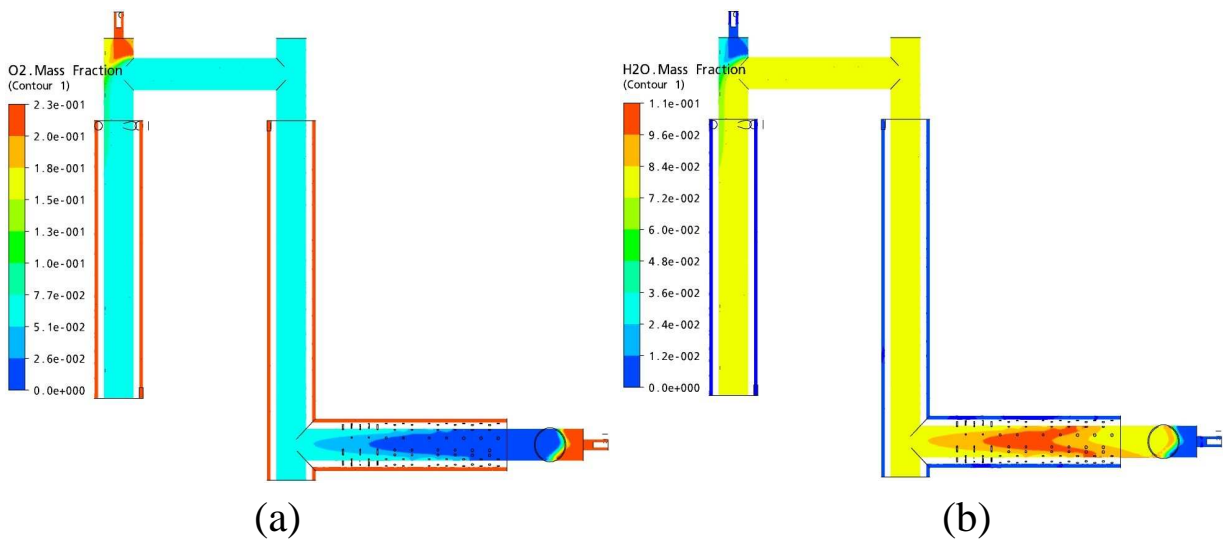


Figure 6 – (a) Oxygen concentration; (b) Water vapor concentration.

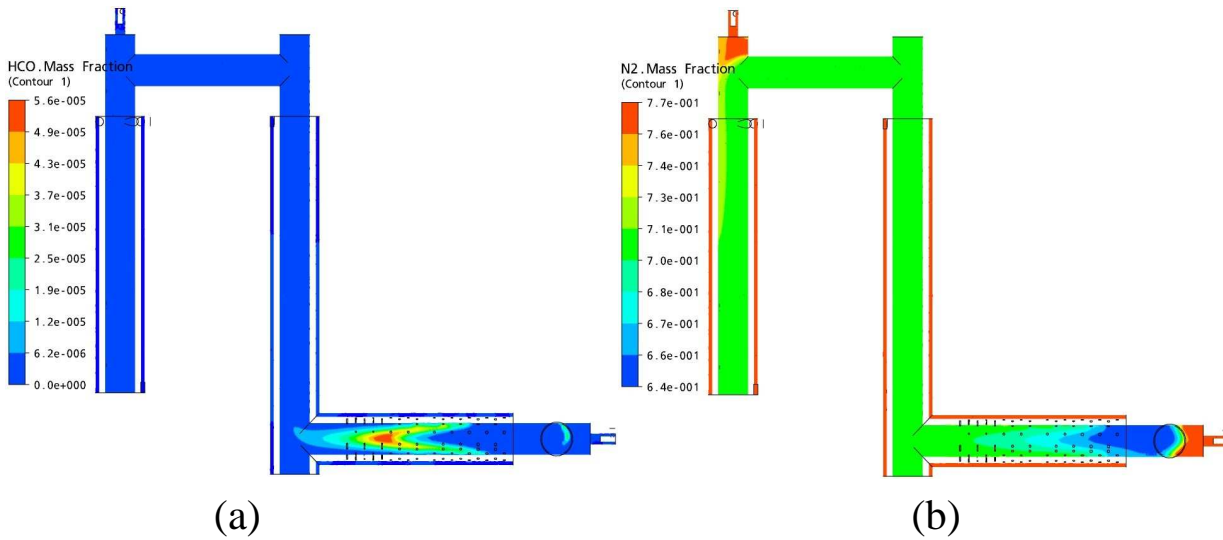


Figure 7 – (a) HCO concentration; (b) Nitrogen concentration.

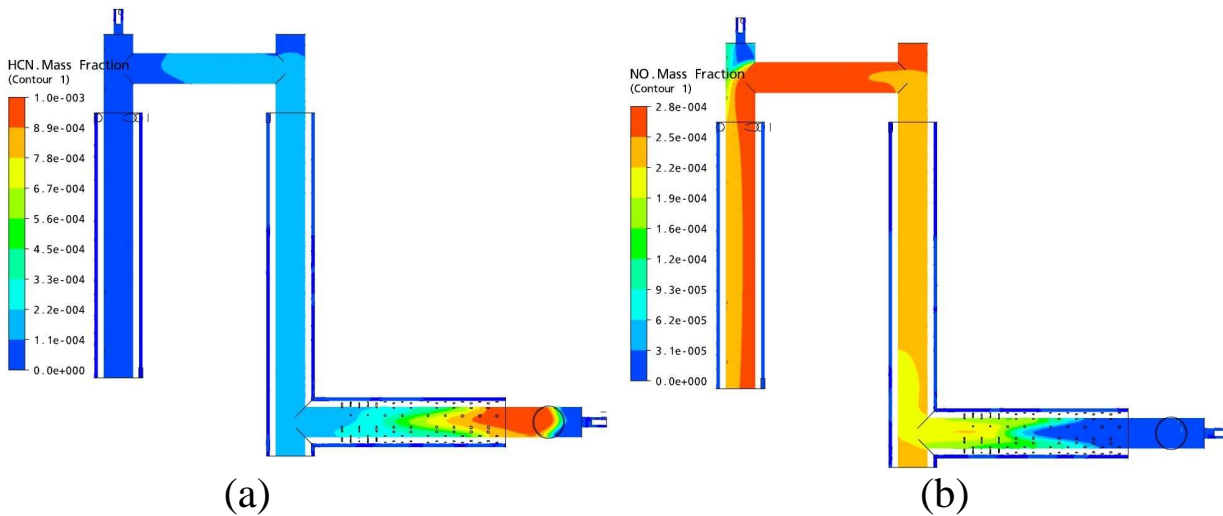


Figure 8 – (a) HCN concentration; (b) NOx concentration.

Figure 8-b shows also that there is a high rate of NO_x formation along the furnace, especially at combustion chamber down flow, where the temperature is the higher one. Indeed, Fig. 2-a shows temperatures on the order of 1300 to

1500 K, high enough to enhance the production of NO_x by the Fennimore mechanism. Besides, one can observe that HCN and NO_x concentrations have an inverse relation; the concentration of one reduces where the concentration of other enhances. The high level of excess air and the large residence time of the flue gases in the furnace also contribute somewhat to the NO_x production.

7. CONCLUSIONS

Analyzing the temperature fields (Fig. 2-a and 3) one can see that the secondary air pre-heater improves substantially the efficiency of the gas burning process, with higher gas temperatures inside the chamber. The higher temperatures along the furnace allowed the installation of the air pre-heater at the segment 4, in order to pre-heat the primary and tertiary air, leading to another improvement of the combustion process. Additionally this second pre-heater generates a supplementary quantity of air to the gasification process, thus enhancing the global efficiency of the plant. Another important conclusion is that the obedience to CONAMA, the Brazilian Counsel of Environment, determinations for CO limits, which determines a high value of excess air, enhances significantly the NO_x production.

8. ACKNOWLEDGEMENTS

The authors thank for the support of CNPq – National Research Council (Brazil) – by granting a research scholarship to the second author.

9. REFERENCES

- Bahillo, A., Armesto, L., Cabanillas, A. and Otero, J., 2004. "Thermal valorization of footwear leather wastes in bubbling fluidized bed combustion". *Waste Management*, Vol. 24, pp. 935-944.
- Carvalho, M.G., Farias, T. and Fontes, P., 1991. "Predicting radiative heat transfer in absorbing, emitting, and scattering media using the discrete transfer method", *ASME HTD*, Vol. 160, pp.17-26.
- CFX Solver Theory, 2004.
- Choi, B.S. and Yi, J., 2000. "Simulation and optimization on the regenerative thermal oxidation of volatile organic compounds". *Chemical Engineering Journal*, Vol. 73, pp. 103-114.
- CONAMA – Conselho Nacional do Meio Ambiente, Ministério do Meio Ambiente, Resolução nº 316, de 29 de outubro do 2002. <<<http://www.mma.gov.br/port/conama/legiabre.cfm?codlegi=338>>>
- Eaton, A. M., Smoot, L. D., Hill, S. C. and Eatough, C. N., 1999, "Components, formulations, solutions, evaluations, and applications of comprehensive combustion models", V. 25, pp. 387-436.
- Fluent User's Guide, vol. 2, 1998.
- Godinho, M., 2006 "Gaseificação e combustão de resíduos sólidos da indústria calçadista". Doctoral Thesis, Programa de Pós-Graduação em Engenharia de Minas, Metalúrgica e de Materiais (PPGEM), Universidade Federal do Rio Grande do Sul, Brazil.
- Godinho, M., Marcilio, N.R., Faria Vilela, A.C., Masotti, L. and Martins, C.B. 2007 "Gaseification and combustion of the footwear leather wastes". *Jalca*, Vol. 102, pp. 182-190
- Kuo, K.K., 1996. "Principles of combustion", John Wiley & Sons, New York.
- Launder, B.E. and Sharma, B.I., 1974. "Application of the energy-dissipation model of turbulence to the calculation of flow near a spinning disc", *Letters in Heat and Mass Transfer*, Vol. 19, pp. 519-524.
- Magnussen B.F. and Hjertager B. H., 1976. "On mathematical models of turbulent combustion with special emphasis on soot formation and combustion". *Proc. of the 16th Int. Symp. on Comb.*, The Combustion Institute, pp. 719-729.
- Salvador, S., Commander, J.M. and Kara, Y., 2006. "Thermal recuperative incineration of VOCs: CFD modeling and experimental validation". *Applied Thermal engineering*, Vol. 26, pp. 2355-2366.
- Shin, D., Yu, T., Yang, W., Jeon, B., Park, S. and Hwang, J., 2008. "Combustion characteristic of simulated gas fuel in a 30 kg/h scale pyrolysis-melting incinerator". *Waste Management*, IN PRESS.
- Spalding, D.B., 1979. "Combustion and Mass Transfer", Pergamon Press, Inc., New York.
- Westbrook, C. K. and Dryer, F.L., 1981. "Simplified reaction mechanisms for the oxidation hydrocarbon fuels in flames". *Comb. Sci. and Technology*, Vol. 27, pp. 31-43.
- Turns, S. T., 2000, "An introduction to combustion – Concepts and applications", 2nd ed, McGraw-Hill, New York.

RESPONSIBILITY NOTICE

The authors are the only responsible for the printed material included in this paper.